

- M. F. Rubner, *Macromolecules* **1998**, *31*, 4309. g) S. S. Shiratori, M. F. Rubner, *Macromolecules* **2000**, *33*, 4213. h) S. L. Clark, M. F. Montague, P. T. Hammond, *Macromolecules* **1997**, *30*, 7237. i) K. Lowack, C. A. Helm, *Macromolecules* **1998**, *31*, 823. j) J. J. Harris, M. L. Bruening, *Langmuir* **2000**, *16*, 2006.
- [16] a) Y. Lvov, K. Ariga, I. Ichinose, T. Kunitake, *J. Am. Chem. Soc.* **1995**, *117*, 6117. b) K. Ariga, Y. Lvov, M. Onda, I. Ichinose, T. Kunitake, *Chem. Lett.* **1997**, 125. c) T. Serizawa, H. Takeshita, M. Akashi, *Langmuir* **1998**, *14*, 4088. d) T. Cassagneau, J. H. Fendler, T. E. Mallouk, *Langmuir* **2000**, *16*, 241. e) E. R. Kleinfeld, G. S. Ferguson, *Science* **1994**, *265*, 370. f) S. L. Clark, E. S. Handy, M. F. Rubner, P. T. Hammond, *Adv. Mater.* **1999**, *11*, 1031. g) N. A. Kotov, I. Dékány, J. H. Fendler, *J. Phys. Chem.* **1995**, *99*, 13065. h) F. G. Aliev, M. A. Correa-Duarte, A. Mamedov, J. W. Ostrander, M. Giersig, L. M. Liz-Marzán, N. A. Kotov, *Adv. Mater.* **1999**, *11*, 1006. i) F. Caruso, H. Möhwald, *Langmuir* **1999**, *15*, 8276. j) F. Caruso, R. A. Caruso, H. Möhwald, *Science* **1998**, *282*, 1111. k) A. Rogach, A. Susa, F. Caruso, G. Sukhorukov, A. Kornowski, S. Kershaw, H. Möhwald, A. Eychmüller, H. Weller, *Adv. Mater.* **2000**, *12*, 333. l) B. J. Battersby, D. Bryant, W. Meutermans, D. Matthews, M. L. Smythe, M. Trau, *J. Am. Chem. Soc.* **2000**, *122*, 2138.
- [17] K.-U. Fulda, A. Kampes, L. Krasemann, B. Tieke, *Thin Solid Films* **1998**, *327-329*, 752.
- [18] R. K. Iler, *J. Colloid Interf. Sci.* **1966**, *21*, 569.
- [19] J. Tien, A. Terfort, G. M. Whitesides, *Langmuir* **1997**, *13*, 5349.
- [20] A. Kampes, B. Tieke, *Mater. Sci. Eng. C* **1999**, *8-9*, 195.
- [21] K. M. Chen, X. Jiang, L. C. Kimerling, P. T. Hammond, *Langmuir* **2000**, *16*, 7825.
- [22] N. G. Hoogveen, M. A. C. Stuart, G. J. Fleer, M. R. Böhmer, *Langmuir* **1996**, *12*, 3675.

## Fabrication of High Performance Ceramic Microstructures from a Polymeric Precursor Using Soft Lithography\*\*

By Hong Yang, Pascal Deschatelets, Scott T. Brittain, and George M. Whitesides\*

This paper describes the fabrication of microstructures and components for microelectromechanical systems (MEMS) made of an oxidation-stable ceramic, borosilicon carbonitride (SiBNC), using soft lithographic techniques. A polymeric precursor **1** is molded into the required form and pyrolyzed to form the ceramic structures. Although shrinkage on pyrolysis is substantial (~30 % in linear dimensions), good retention of relative geometry is observed. The density of the structures obtained after pyrolysis under argon is  $\rho = \sim 1.8 \text{ g/cm}^3$ . These ceramic microstructures withstand temperatures  $>1050^\circ\text{C}$  in air for times  $>2 \text{ h}$ . This oxidation stability is one of the several advantages of SiBNC as a material.

An important problem in MEMS is the development of materials that can tolerate high temperatures and oxidizing

environments. The range of materials suited for high-temperature applications is limited, and only a few can maintain their mechanical strengths at temperatures exceeding  $1300^\circ\text{C}$ .<sup>[1]</sup> Silicon carbide (SiC)<sup>[2]</sup> and silicon nitride ( $\text{Si}_3\text{N}_4$ )<sup>[3]</sup> are the best explored examples. These materials suffer from drawbacks: they are difficult to fabricate, they undergo phase transformations, and they degrade mechanically at temperature  $\geq 1400^\circ\text{C}$ . The metal alloys used in current gas-turbine engines (e.g., NiAl-based materials) fail mechanically, or begin to melt at  $1395^\circ\text{C}$ .<sup>[4]</sup>

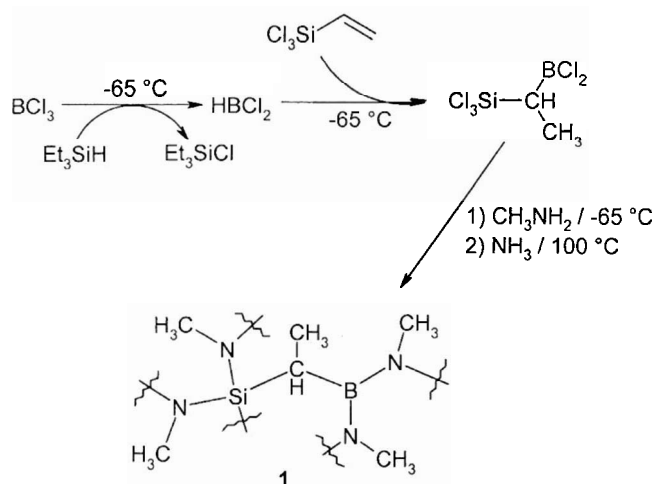
Borosilicon carbonitride (SiBNC) quaternary ceramics can be synthesized from several preceramic polymers.<sup>[5-10]</sup> The SiBNC ceramics made from different precursors can have quite different properties. The quaternary ceramics of this sort synthesized by Jansen and co-workers are claimed to retain a dense amorphous form at temperatures exceeding  $2000^\circ\text{C}$ , and are stable at that temperature in an inert atmosphere.<sup>[7]</sup> Some other types of SiBNC ceramics are reported to show excellent resistance to oxidation, and to be stable in air up to  $1500^\circ\text{C}$ . Their fully dense form still retains a low density ( $\rho = \sim 1.8 \text{ g/cm}^3$ ).<sup>[1]</sup> This combination of properties is attractive in applications such as gas turbines, where light weight and high-temperature ( $>1450^\circ\text{C}$ ) oxidative stability are attractive.<sup>[11]</sup> This ceramic, formed by pyrolysis of melt-spun fiber, has been commercialized by Bayer as Siboramic.<sup>[1,12,13]</sup> Practical methods of making functional structures of the sorts required for high-temperature MEMS remain to be developed.

Most current MEMS devices are made of silicon.<sup>[14,15]</sup> Conventional photolithography, coupled with surface machining, is the most commonly used method to obtain the micrometer-sized surface features required for sensors and actuators. LIGA (lithographic, galvanoförmung, abförmung)<sup>[16]</sup> has been used to fabricate MEMS components with high aspect ratios made of materials other than silicon, and has been examined for the fabrication of ceramic microstructures from polymeric precursors.<sup>[17]</sup> The applications of this technique are limited because it requires access to a synchrotron source. The fabrication of technologically important ceramic materials (especially silicon carbide) is most frequently done using reactive ion etching (RIE). New methods such as ink-jet printing<sup>[18,19]</sup> and injection molding of a preform<sup>[20]</sup> are also being explored for other ceramic materials, such as ceramic powders, nanostructured composites, and SiCN.

Soft lithography is a set of techniques that offers simple routes to microstructures formed from polymers. By using polymers that are precursors of ceramics,<sup>[21]</sup> it is possible to use soft lithographic techniques to generate complex ceramic features without resorting to etching procedures.<sup>[22,23]</sup> We used the moldable single-source polymer **1**, originally described by Jansen and co-workers, as our ceramic precursor (Scheme 1).<sup>[7,24]</sup> Microtransfer molding ( $\mu\text{TM}$ )<sup>[25]</sup> and vacuum assisted micromolding in capillaries (MIMIC)<sup>[26]</sup> were used to fabricate test structures: hexagonal honeycomb microstructures, and preforms for microgears (Fig. 1). We conclude that these methods provide practical approaches to micrometer-sized features of SiBNC with aspect ratios  $\geq 3$ . The final

[\*] Prof. G. M. Whitesides, Dr. H. Yang, Dr. P. Deschatelets, Dr. S. Brittain  
Department of Chemistry and Chemical Biology  
Harvard University  
12 Oxford Street, Cambridge, MA 02138 (USA)  
E-mail: gwhitesides@gmgroup.harvard.edu

[\*\*] This work was supported by Defense Advanced Research Program Agency (DARPA) and National Science Foundation (NSF ECF-9729405). We thank Dr. Bob Chapman, Dr. Noo Li Jeon, Mr. Tao Deng, and Dr. Jason Wiles for their help. We are grateful to Dr. Yuan Lu for the XPS analysis. H. Y. thanks the Natural Sciences and Engineering Research Council (NSERC) of Canada for a postdoctoral fellowship. P. D. thanks Les Fonds pour la Formation de Chercheurs et l'Aide à la Recherche (FCAR) for a postdoctoral fellowship.



Scheme 1. Synthesis of preceramic polymer **1** [7].

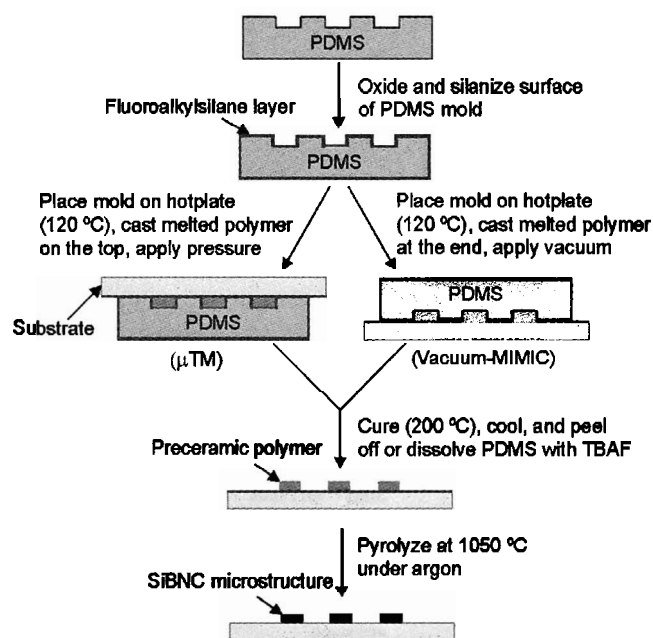


Fig. 1. Schematic illustration of procedures for fabrication of the ceramics using  $\mu$ TM and vacuum-assisted MIMIC of the preceramic polymer.

SiBNC ceramic microstructures were obtained after pyrolysis of the preceramic polymer.

Figure 1 summarizes the process used for the fabrication of ceramic microstructures. In this procedure, for isolated or discontinuous structures, a polydimethylsiloxane (PDMS) mold was filled with melted preceramic polymer **1**. A silicon wafer substrate was pressed against the filled PDMS mold using a pressure of  $\sim 5$  psi ( $\sim 3 \times 10^4$  Pa). Vacuum-assisted MIMIC<sup>[26]</sup> was used as an alternative for fabrication of continuous microstructures such as honeycombs. In this case, the channels were filled with the polymer by capillary flow and assisted by applying vacuum in the channels. The preceramic polymer was then cured at 200 °C for  $\sim 1$  h, and the mold was removed either by peeling it off from the substrate or by dissolving it in a solution of 1.0 M tetrabutylammonium fluoride (TBAF) in tetrahydro-

furan (THF) at room temperature.<sup>[27]</sup> These polymeric microstructures were placed on top of a silicon substrate and transferred into a tube furnace. The temperature of the furnace was increased to  $>1050$  °C at a rate  $\leq 2$  °C/min. Low molecular weight gases (e.g., methylamine, methane, and HCN; caution: some of these gases are very toxic, and the pyrolysis should be conducted in a fumehood) were slowly released from the polymer over the temperature range from  $\sim 150$  °C to  $\sim 700$  °C during the pyrolysis.<sup>[7]</sup> The fact that gas evolution occurs slowly may help to prevent the ceramics from forming large voids, and from cracking due to such defects. The polymeric structures were converted into ceramics at  $>1050$  °C.

Figure 2 shows scanning electron micrographs (SEM) of SiBNC ceramic hexagonal microstructures. We chose channel widths ranging from  $\sim 25$ – $30$   $\mu$ m to  $100$   $\mu$ m for these structures because these sizes are representative of those used for MEMS devices, and because the masks required to make molds of the appropriate structures can be generated easily using rapid prototyping.<sup>[28]</sup> Before pyrolysis, the microstructures of preceramic polymer are optically transparent and sensitive to moisture. Upon pyrolysis at  $\sim 1050$  °C for  $>2$  h, the microstructures turned lustrous black and became stable in air. We estimate the density of the final product to be  $\sim 1.8$  g/cm<sup>3</sup>, since the ceramics have a density similar to that of perfluorononane ( $\rho = 1.799$  g/cm<sup>3</sup>).<sup>[29]</sup> The widths of the hexagonal walls are  $\sim 20$   $\mu$ m and  $70$ – $72$   $\mu$ m for the honeycombs made from molds with channel widths of  $\sim 30$   $\mu$ m and  $100$   $\mu$ m. These final values correspond to a lateral contraction of  $\sim 30\%$ , a value that agrees with that reported for the bulk material.<sup>[7]</sup> Figure 2D is a side view of the ceramic honeycomb structures made from PDMS molds having a channel width of  $\sim 30$   $\mu$ m. We obtained aspect ratios in the order of 2–3:1 (Fig. 2B), but we believe that larger values can be obtained. After the pyrolysis of the polymeric features, the final ceramic microstructures either remained attached to the substrates as shown in Figure 2A and 2B, or released spontaneously from the substrates as free-standing honeycombs as shown Figure 2C and 2D. Structures that released spontaneously did so, we presume, as a result of stress accumulated during pyrolysis and shrinkage.

Figure 2E–G demonstrate the high-temperature oxidation stability of these structures. Figure 2E and 2F show the same area of a hexagonal microstructure before and after exposure to air for 2 h at  $1050$  °C. Those two electron micrographs were taken from the same areas of the same free-standing honeycomb. A micrograph at high magnification (Fig. 2G) shows that the walls of hexagons are smooth and without obvious defects. These observations indicate that the form of the molded ceramics is retained after exposure to the air at high temperature. Defects such as pinholes were sometimes observed in final structures. We believe that these defects were caused by imperfect filling of the channels, and by a low degree of polycondensation of the preceramic polymer, but we have not yet optimized the process.

Figure 3 demonstrates fabrication of a structure with a more complex shape: a microgear. The aspect ratio of the

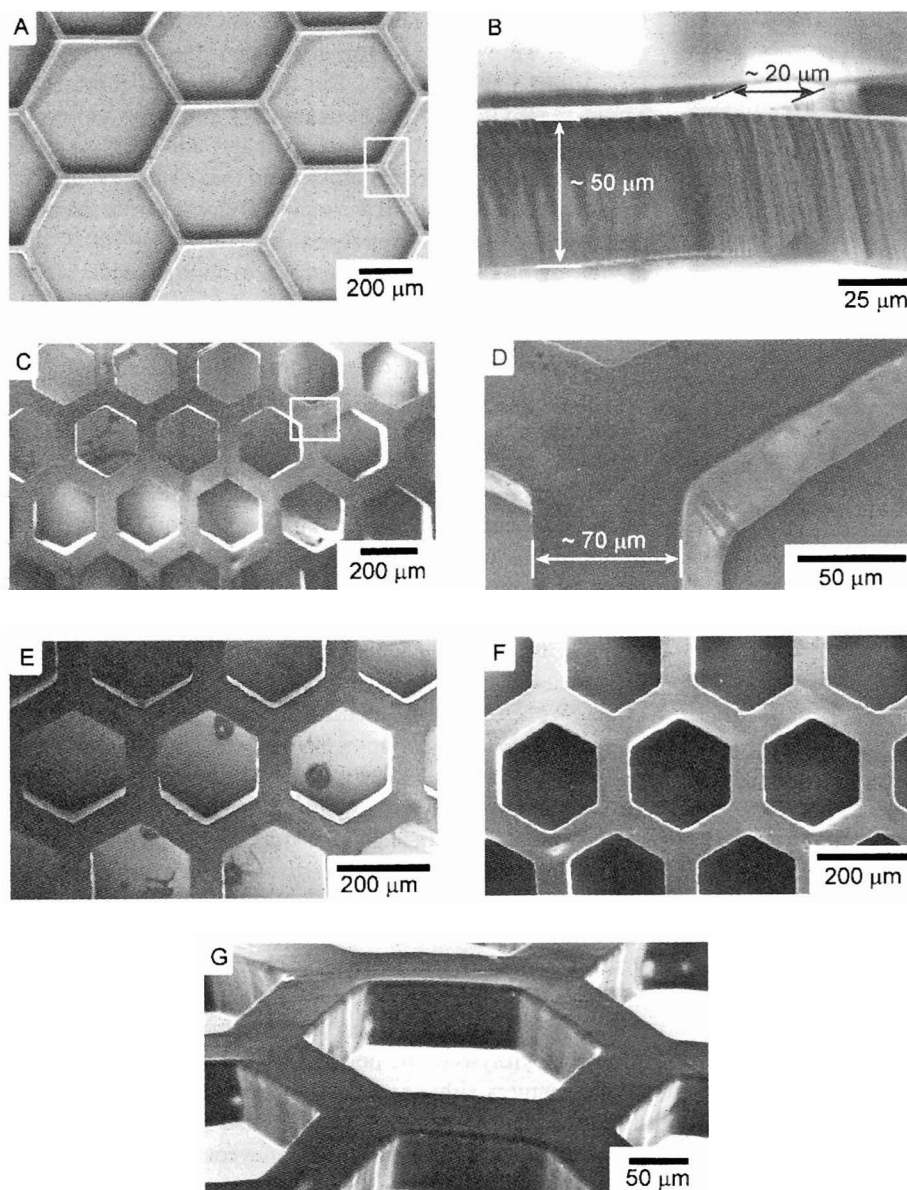


Fig. 2. SEM images of hexagonal grids of SiBNC ceramics. The widths of the hexagonal walls are A)–B)  $\sim 20\ \mu\text{m}$  and C)–D)  $70\ \mu\text{m}$ ; E) ceramic structure at a tilt of  $\sim 15^\circ$  to the image stage; F) the same structure after exposure to air at  $1050^\circ\text{C}$  for 2 h; G) sample as in F) at higher magnification and a tilt of  $60^\circ$  to the image stage.

teeth in this particular design is  $\sim 3\text{--}4\text{:}1$  (Fig. 3B). The high magnification SEM of the hole shows a smooth surface. This observation implies that the preceramic polymer replicates the molds with high fidelity (Fig. 3C). We observed cracking lines on the thin surface layer; those lines were limited to the surface, and did not advance into the structure. Examination of the surface of the ceramic samples by X-ray photoelectron spectroscopy (XPS) showed that the surface elemental composition is 31 % Si, 8 % B, 11 % C, and 50 % O; these values correspond to a surface composition of  $\text{SiB}_{0.3}\text{C}_{0.4}\text{O}_{1.6}$ . The element composition of the interior of the ceramic material was also examined using a freshly-fractured surface by XPS. This surface is composed of 19 % Si, 11 % B, 18 % N, 23 % C, and 28 % O, which corresponds to an internal composition of  $\text{SiB}_{0.6}\text{N}_{0.93}\text{C}_{1.2}\text{O}_{1.5}$ . We attribute the high oxygen content of these samples to the fact that we did not handle the preceramic polymer in an environment free of oxygen or moisture;<sup>[3]</sup>

The oxygen content could, we presume, be substantially reduced by manipulations in a dry box. The loss of elements having volatile oxides (B, N, and C) from the surface during the pyrolysis may result in shrinking and surface cracking.

In conclusion, soft lithography provides a route to microstructures of SiBNC. The microstructures made from this material are potentially important for high temperature MEMS applications. We expect SiBNC ceramic microstructures to find applications in devices that are required to withstand harsh oxidative and thermal environments, such as microcombustors, microturbines, high-temperature sensors and actuators, and microchemical reactors.<sup>[30,31]</sup> This demonstration has focused on the SiBNC class of preceramic polymers. A wide range of polymeric precursors to ceramics have, of course, been developed.<sup>[3,6,32]</sup> The methods described here should be applicable to these materials as well.

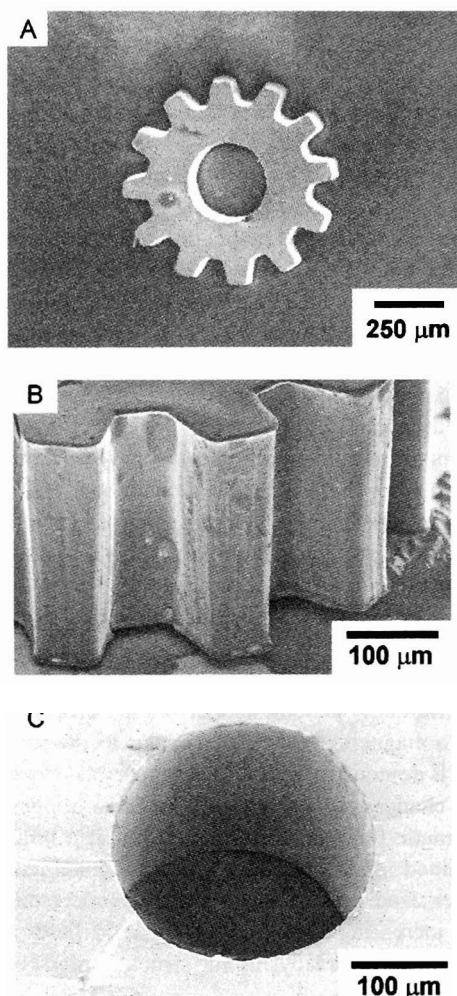


Fig. 3. SEMs of a free-standing micrometer-sized gear of SiBNC ceramic made by using  $\mu$ TM: A) top view of the gear; B) side view of the teeth, and C) side view of the hole. After curing at 200 °C for 1 h and cooling to room temperature, the polymeric gear was immersed in a TBAF solution in THF for ~30 min. During this treatment, the gear was first released from the silanized substrate and then the PDMS mold was slowly dissolved. The free-standing polymeric gear was subsequently placed on a silicon substrate, transferred into a quartz tube furnace and converted into ceramic by pyrolysis.

## Experimental

**Fabrication of Elastomeric PDMS Molds and Treatment of Substrates:** The photomasks used for the fabrication of masters were transparency films having opaque patterns of features printed by a high-resolution printer ( $\geq 3386$  dpi) [28]. The masters were fabricated using SU-8 photoresist (MicroChem Corp., Newton, MA; [www.microchem.com](http://www.microchem.com)) on silicon wafers (Test grade, Silicon Sense, Inc., Nashua, NH; [www.siliconsense.com](http://www.siliconsense.com)) by conventional photolithographic techniques. The bas-relief masters of SU-8 were silanized in a desiccator that was connected to house vacuum, and contained a vial with small amount of (tridecafluoro-1,1,2,2-tetrahydrooctyl)-1-trichlorosilane (United Chemical Technology, Bristol, PA; [www.unitedchem.com](http://www.unitedchem.com)). The silanization was used to prevent adhesion of PDMS to the masters. Casting prepolymer, Sylgard 184 (Dow Corning, Midland; [www.dowcorning.com](http://www.dowcorning.com)) on these silanized masters and curing at 70 °C formed the PDMS molds with bas-relief structures as negative replicas of the structures in the SU-8. The PDMS molds were heated at 160 °C in an oven for ~2 h to complete the cure. The surface of the PDMS mold was oxidized with oxygen plasma in a plasma cleaner (SPI Plasma PREP II; [www.2spi.com](http://www.2spi.com)) at a pressure of ~1 mm Hg for 2 min. These molds were then exposed to vapors of (tridecafluoro-1,1,2,2-tetrahydrooctyl)-1-trichlorosilane for ~12 h to obtain hydrophobic surfaces. Polished silicon wafers were used as

substrates and treated with oxygen plasma and silanized by the aforementioned reagent prior to use.

**Synthesis of Polymeric Precursor:** All syntheses were performed under an argon atmosphere in Schlenk-type glassware. The polymeric precursor was synthesized from 1-(trichlorosilyl)-1-(dichloroboryl)ethane (TSDE) following a general scheme described by Jüngermann et al. [7,24]. We adjusted the duration of the polymerization under an ammonia atmosphere in order to obtain a preceramic polymer with a suitable viscosity for  $\mu$ TM and vacuum assisted MIMIC at temperatures of 120–140 °C. The product was a colorless transparent glass-like solid at room temperature. At 120 °C, the preceramic polymer has a viscosity similar to that of thick honey.

**Synthesis of TSDE:** Boron trichloride (99.9 %, Aldrich, 0.1 mol, ~9 mL at –78 °C) was condensed at –65 °C in a round-bottom flask equipped with an addition funnel. Trichlorovinylsilane (97 %, Aldrich, 0.1 mol, ~13 mL) was premixed with triethylsilane (99 %, Aldrich, 0.1 mol, ~16 mL), and added dropwise to  $\text{BCl}_3$  over 15 min. The mixture was stirred for 1 h and then allowed to warm to room temperature. The reaction mixture was distilled using a Vigreux column at –40 °C/12 mbar to obtain TSDE. The product is a colorless liquid at room temperature and extremely sensitive to moisture and air. (Caution:  $\text{BCl}_3$  is highly corrosive and should be handled with care.)

**Synthesis of the Preceramic Polymer 1:** TSDE (~0.06 mol) was added dropwise to a solution of ~60 mL of methylamine (anhydrous, 98+ %, Aldrich) in ~180 mL of dry hexane (100.0 %, A.C.S. reagent, J. T. Baker, Phillipsburg, NJ) at –65 °C under argon. The mixture was allowed to react overnight under vigorous stirring. After reaction was complete, the mixture was warmed to room temperature, and a white solid was removed by filtration using house vacuum. Hexane was removed by distillation from the filtrate using a rotary evaporator (Model: R110, Büchi) under moderate vacuum (~20 mm Hg). This polymer was heated for 1–2 h at 100 °C under an atmosphere of ammonia, followed by degassing under vacuum (~3 mm Hg) for 30 min. Upon cooling to room temperature, a colorless glassy solid was obtained and stored under argon.

**Fabrication of Microstructures of SiBNC Ceramics:** The manipulations were conducted in a glove bag under argon. The fabrication of preceramic microstructures using  $\mu$ TM involves the following steps: i) Silanized PDMS molds were placed on a hot plate with their structured surface facing upward. The temperature of the hotplate was set at 120 °C. ii) A flask containing preceramic polymer 1 was heated on the hotplate. After this polymer melted into a viscous liquid, it was transferred onto the top of the molds using a spatula. iii) After the polymer filled the voids of the PDMS mold, a silanized silicon wafer was placed on the top. A pressure of ~5 psi ( $\sim 3 \times 10^4$  Pa) was applied on the wafer using a weight. iv) The temperature of the hotplate was then raised to 200 °C at a rate of 2 °C/min. The polymer was cured at this temperature for 1 h and cooled to room temperature on the hotplate. An alternative process used vacuum assisted MIMIC [26]. In this method, a PDMS mold was placed directly against the surface of a silanized silicon substrate on a hotplate. The preceramic polymer was melted at 120 °C and transferred to the entrance of the PDMS mold using a spatula. The channels were filled with the polymer by applying vacuum in the channels and by capillary flow. The hotplate was heated to 200 °C, held at that temperature for 1 h, and cooled to room temperature.

Once the hotplate was cooled down, we first tried to peel off the PDMS mold from the silanized substrate and from the preceramic microstructure. The mold could sometimes be removed from the substrate, leaving the preceramic microstructures still attached to the silicon substrate. In these cases, the preceramic structures along with the substrate were transferred into a quartz tube furnace for the pyrolysis. When the PDMS molds could not be peeled off from the polymeric microstructures, we used a 1.0 M TBAF solution in THF (Aldrich) to dissolve the PDMS mold. In this case, the microstructure and the PDMS mold were normally released from the silanized substrate first. The preceramic microstructure became free-standing after the dissolution of the PDMS mold by the TBAF solution. This free-standing preceramic structure was placed on top of a silicon substrate and transferred into the quartz tube furnace for pyrolysis.

The conversion of polymeric microstructures into ceramics started with the purge of the samples positioned in the center of a quartz tube with argon for ~15 min. The temperature of the furnace (model: TF55035A, Linderberg/Blue) was raised to 1050 °C at a rate of 1 °C/min and held for 2 h at that temperature. After the pyrolysis, the furnace was cooled to room temperature at a rate of 2 °C/min. If the preceramic structures were free-standing, the final ceramic structures could be easily removed from the silicon substrate. Some microstructures that were initially attached to the silanized silicon substrate released spontaneously, we presume, as a result of stress accumulated during pyrolysis and shrinkage. The test of thermal stability of the ceramic microstructure was performed using a free-standing microstructure of hexagonal honeycomb grid following a similar pyrolysis procedure but in air.

Received: July 4, 2000  
Final version: August 24, 2000

- [1] P. Baldus, M. Jansen, D. Sporn, *Science* **1999**, *285*, 699.
- [2] M. Mehregany, C. A. Zorman, N. Rajan, C. H. Wu, *IEEE* **1998**, *86*, 1594.
- [3] R. Riedel, in *Processing of Ceramics Part II*, Vol. 17B (Ed: R. J. Brook), VCH, Weinheim **1996**, p. 1.
- [4] D. P. Pope, R. Darolia, *MRS Bull.* **1996**, *21*, 30.
- [5] H.-P. Baldus, O. Wagner, M. Jansen, *Mater. Res. Soc. Symp. Proc.* **1992**, *271*, 821.
- [6] H.-P. Baldus, M. Jansen, *Angew. Chem. Int. Ed. Engl.* **1997**, *36*, 328.
- [7] H. Jüngermann, M. Jansen, *Mater. Res. Innovat.* **1999**, *2*, 200.
- [8] M. Weinmann, J. Schuhmacher, H. Kummer, S. Prinz, J. Peng, H. J. Seifert, M. Christ, K. Müller, J. Bill, F. Aldinger, *Chem. Mater.* **2000**, *12*, 623.
- [9] T. Wideman, K. Su, E. E. Remsen, G. A. Zank, L. G. Sneddon, *Chem. Mater.* **1995**, *7*, 2203.
- [10] R. Riedel, A. Kienzie, W. Dresser, L. Ruwisch, J. Bill, F. Aldinger, *Nature* **1996**, *382*, 796.
- [11] D. Hull, T. W. Clyne, *An Introduction to Composite Materials*, Cambridge University Press, Cambridge **1996**.
- [12] H.-P. Baldus, G. Passing, H. Scholz, D. Sporn, M. Jansen, J. Goring, *Key Eng. Mater.* **1997**, *127–131*, 177.
- [13] H.-P. Baldus, G. Passing, A. Eiling, Bayer Aktiengesellschaft, *US Patent* 5985 430, **1999**.
- [14] M. Madou, *Fundamentals of Microfabrication*, CRC Press, New York **1997**.
- [15] G. T. Kovacs, *Micromachined Transducers Sourcebook*, McGraw-Hill, New York **1998**.
- [16] H. Guckel, *IEEE* **1998**, *86*, 1586.
- [17] H. Freimuth, V. Hessel, H. Kölle, M. Lacher, W. Ehrfeld, *J. Am. Ceram. Soc.* **1996**, *79*, 1457.
- [18] M. Mott, J. H. Song, J. R. G. Evans, *J. Am. Ceram. Soc.* **1999**, *82*, 1653.
- [19] H. Fan, Y. Lu, A. Stump, S. T. Deed, T. Baer, R. Schunk, V. Perez-Luna, G. P. Lopez, J. C. Brinker, *Nature* **2000**, *405*, 56.
- [20] L. An, W. Zhang, V. M. Bright, M. L. Dunn, R. Raj, *IEEE Conference on Micro Electro Mechanical Systems (MEMS 2000)*, Miyazaki, Japan, Jan 23–27 **2000**.
- [21] C. Marzolin, S. P. Smith, M. Prentiss, G. M. Whitesides, *Adv. Mater.* **1998**, *10*, 571.
- [22] Y. Xia, G. M. Whitesides, *Angew. Chem. Int. Ed.* **1998**, *37*, 550.
- [23] B. A. Grzybowski, S. T. Brittain, G. M. Whitesides, *Rev. Sci. Instrum.* **1999**, *70*, 2031.
- [24] M. Gastreich, C. M. Marian, H. Jüngermann, M. Jansen, *Eur. J. Inorg. Chem.* **1999**, 75.
- [25] X.-M. Zhao, Y. Xia, G. M. Whitesides, *Adv. Mater.* **1996**, *8*, 837.
- [26] N. L. Jeon, I. S. Choi, B. Xu, G. M. Whitesides, *Adv. Mater.* **1999**, *11*, 946.
- [27] E. J. Corey, A. Venkateswarlu, *J. Am. Chem. Soc.* **1972**, *94*, 6190.
- [28] D. Qin, Y. Xia, G. M. Whitesides, *Adv. Mater.* **1996**, *8*, 917.
- [29] *Aldrich Handbook of Fine Chemicals and Laboratory Equipment*, Milwaukee **2000–2001**.
- [30] K. F. Jensen, *AIChE J.* **1999**, *45*, 2151.
- [31] R. Srinivasan, I. M. Hsing, P. E. Berger, K. F. Jensen, S. L. Firebaugh, M. A. Schmidt, M. P. Harold, J. J. Lerou, J. F. Ryley, *AIChE J.* **1997**, *43*, 3059.
- [32] M. Jansen, H. Jüngermann, *Curr. Opin. Solid State Mater. Sci.* **1997**, *2*, 150.

## Domain Shapes and Superlattices Made of Cobalt Nanocrystals

By Julie Legrand, Ahn-Tu Ngo, Christoph Petit, and Marie-Paule Pileni\*

In recent years, ferromagnetic nanomaterials have received considerable attention, both theoretically and experimentally, owing to their potential applications and their extraordinary behavior. The behavior of isolated magnetic nanoparticles has

been extensively studied and is well understood.<sup>[1]</sup> However, when such particles are agglomerated in dense systems such as granular films, the magnetic properties differ significantly from the individual and bulk properties. There are numerous results for granular magnetic solids,<sup>[2]</sup> but no results for 3D superlattices. This is partly due to the difficulty of making such 3D patterns of well-organized magnetic nanocrystals on a sufficiently large scale. Collective magnetic properties were recently reported for nanocrystals self-organized in 2D hexagonal networks.<sup>[3,5]</sup> For magnetic nanoparticles, 3D organization has not yet been observed on a very large scale, even if they self-assemble in a 2D network, whereas metal nanocrystals with the same diameter and size distribution self-assemble in 3D face-centered cubic (fcc) structures.<sup>[4,6]</sup> Formation of “pseudo-crystals” made of individual magnetic nanoparticles will open a fascinating new field of physical chemistry. These artificial structures can be manipulated to achieve tailored materials for applications and for exploration of physical phenomena, as the magnetic properties of this new class of materials should differ both from those of individual nanoparticles and bulk materials.

The aim of this communication is to report the formation of large-scale 3D superlattices of cobalt nanocrystals. During the deposition process a magnetic field perpendicular to the substrate is applied. It is demonstrated that the nanocrystal organization markedly changes with the strength of the applied field. With no magnetic field, no 3D superlattices at a large scale could be obtained. At low applied fields, hexagonal patterns of micrometer-sized dots made of cobalt nanocrystals are observed. On increasing the applied magnetic field, a phase transition from dots to a labyrinthine structure made of cobalt nanocrystals takes place.

The synthesis of coated cobalt nanocrystals of 8 nm diameter, 14 % size distribution, and dispersed in hexane is described below. To grow 3D superlattices of cobalt nanocrystals, the evaporation rate has to be very slow. The procedure is as follows: a freshly cleaved highly oriented pyrolytic graphite (HOPG) substrate is immersed in 200  $\mu\text{L}$  of  $4 \times 10^{-7}$  M nanocrystals dispersed in hexane. The evaporation process, which takes 12 h, occurs under hexane vapor and produces a black magnetic film. The amount of material deposited on the substrate is around 40 % of the initial mass. This is deduced from the optical density at 650 nm of nanocrystals collected from the substrate and dispersed in hexane.

An external magnetic field perpendicular to the substrate is applied during the deposition process. It is expected that each nanocrystal moment is aligned in the field direction. Figure 1 shows the variety of structures made of cobalt nanocrystals depending on the strength of the field. Addition of a hexane drop to the substrate totally destroys these structures. A drop of this solution is deposited on a transmission electron microscopy (TEM) grid. The pattern clearly shows well-defined nanocrystals, which are partially self-assembled in 2D superlattices.<sup>[7]</sup> The UV spectrum and magnetic hysteresis loop of nanocrystals collected from the substrate and dispersed in hexane remain unchanged compared to those observed before

\* Prof. M. P. Pileni, Dr. J. Legrand, Dr. A. T. Ngo, Dr. C. Petit  
Université P. et M. Curie, Laboratoire SRSI, URA CNRS 1662  
4 Place Jussieu, 75251 Paris Cedex (France)  
E-mail: pileni@sri.jussieu.fr